Multifunctional Current-Controlled DSTATCOM with Harmonic Mitigation Through Voltage Detection

Jean C. da Cunha*, Sérgio V. G. Oliveira*, Leandro Michels† and Marcello Mezaroba*
*Santa Catarina State University, Joinville, Brazil, 89220–500
Email: cunha.jeanc@gmail.com, sergio_vidal@ieee.org, marcello.mezaroba@udesc.br
†Santa Maria Federal University, Santa Maria, Brazil, 97105–900
Email: michels@ieee.org

***Abstract*—This paper presents a control scheme for Static Compensators applied in distribution systems (DSTATCOM), that are used for regulation of voltage magnitude at point of common coupling (PCC) and it also has the function of eliminating harmonics of voltage through PCC-voltage-detection method. Voltage-magnitude regulation is accomplished through quadrature-current injection at PCC and harmonic mitigation is released reading the voltage at PCC and producing harmonic currents capable of voltage-distortion compensation at PCC. Using this method there is not necessity of source or load-current measurement. The voltage regulator was implemented using a four-wire three-phase shunt-connected VSI. Consumption of active power is needed to compensate converter's losses and regulate dc-link voltage. Simulation and preliminary experimental results of the complete system are presented to demonstrate the effectiveness of the solution.**

I. Introduction

The quality of consumer voltage in Brazil is regulated by the National Agency of Electric Energy (ANEEL) through a set of documents called Distribution Proceedings (PRODIST) [1], hence the magnitude of grid voltage as well as its harmonic content must be kept in adequate levels, as it was previewed by IEEE 519 [2]. Nowadays ANEEL obligates consumer refunding by power distributors in case of voltage-magnitude inadequacy at the point of common coupling (PCC), but the emergence of a similar policy about harmonic content is expected.

Aiming to adequate voltage quality, solutions as improvement of infrastructure, usage of grid-connected passive elements and changes in transformer's TAPs are natural but they require an extensive planning by distributors, which may delay more than ANEEL term, costing them extra expenses. This paper suggests a temporary solution, overcoming voltage-quality problem while a definitive solution is prepared, therefore avoiding refunds by distributors and quickly solving the consumers' problem. The solution must deal with fast implementation, easy installation and low volume. It is called Mobile Voltage-Quality Regulator (MVQR) and after implanting a permanent solution this device can be moved to another problematic PCC.

Active solutions which were implemented in transmission and distribution systems are able to increase systems' power-transmission capability, voltage quality and stability [3], [4].

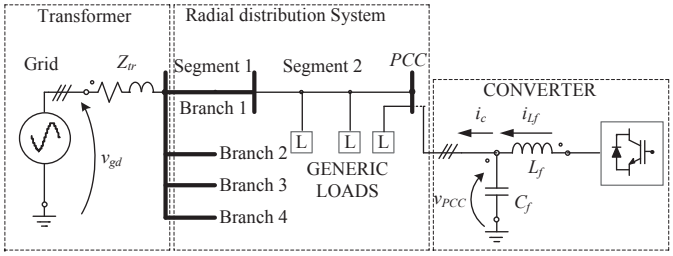

Fig. 1. General structure of the system, illustrating a possible PCC where the MVQR is connected.

Due their flexibility, they can bear multifunctions [4]–[6] as in distributed generation (DG) systems.

Processing only reactive power the MVQR implementation becomes feasible, dealing with weight and volume reduction and dispensing external power sources. Also, it is distribution-grid shunt connected because breaking the distribution line may turn its installation more complex, more time consuming and less reliable. All these features are found in synchronous static compensators (STATCOM) [7], distribution STATCOMs (DSTATCOM) [8], [9], active power filters (APF) with reactive compensation [10]–[22] and multifunctional converters [4]–[6], [23]–[30], including DG systems. Often, differences among these converters are only their main duty [10], once slight modifications on their control schemes can change or upgrade their duties. MVQR has regulation of PCC-voltage magnitude as priority, so that being classified as DSTATCOM with the multifunctional feature of voltage-harmonic mitigation.

MVQR is implemented using a three-phase four-wire VSI converter to regulate temporarily v_{PCC} quality in a distribution grid of the Brazilian scenario, extending distributor term for implementation of a permanent solution. The converter can be connected to any point of distribution grid, not necessarily at the same point of the problematic load. It also must regulate v_{PCC} voltage magnitude into 3 seconds, according to [1]. General structure of this system is shown in Fig. 1.

Section II presents the control strategy and its design, where in Section II-D interaction among all control loops is explored. In the following, Section III presents the effectiveness of the control technique bringing experimental results from

laboratory. Conclusions are drawn in section V.

II. Control Strategy

Control strategies of DSTATCOM can be classified as either current controlled or voltage controlled. In voltage control [23], [26] there is natural regulation of both voltage magnitude and v_{PCC} harmonics, nevertheless there is not natural current (i_{Lf}) limitation, decreasing converter robustness during transients. There are techniques to protect indirectly the converter against overloads [23], [26], [31] but they need foreknowledge of grid's equivalent impedance or even they need insertion of an extra series impedance between grid and converter [4]. This paper prioritizes robustness of this application hence it uses current control, where even under large v_{PCC} variations L_f-inductor current (i_{Lf}) is kept limited by simply limiting current references.

Harmonic-mitigation strategies can be classified as load-current detection, source-current detection or voltage detection [15]. This paper uses the voltage-detection method once MVQR is enabled to compensating voltage harmonics only near the source of harmonics, because this source may not be easily detected by a distribution company (see Fig. 1). This scenario turns the harmonic mitigation through current detection unfeasible.

Harmonic mitigation using v_{PCC} detection can be implemented through emulation of resistances for harmonics, actively damping harmonics [15], [17], [24], [32], but this method does not envisage complete elimination of harmonics. Emulation of tuned active filters was done by [19], however these filters can resonate with non-foreseen loads [22]. With similar features to voltage controlled converters, but current controlled, there are solutions that use non-linear and adaptive techniques [6], [28], [29], [33], but some of them have chattering problem and they aggregate higher complexity comparing with linear techniques. In this paper is not expected the compensation of non-periodic v_{PCC} distortions and those techniques do not become attractive.

Harmonics can be mitigated using internal-model based controllers as resonant [10], [27], [34] and repetitive structures [14], which are also applied in current control because of their good reference tracking and good rejection of periodic disturbances. This paper uses resonant controllers for harmonic compensation, acting only in chosen frequencies, not acting in zero and fundamental frequencies.

The used control strategy is presented in Fig. 2, being similar to [35] but differentiating by addition of harmonic loops and by consideration of parametric variation of grid's model in controller designs. The v_{PCC} sampling circuit has anti-alias filters (f_{aa}). For the generation of sinusoidal references, effective v_{PCC} values and i_h^* signals there are conventional types of digital analog signal converters (DAC) and types that use pwm with high frequency filters f_{DA}. Sinusoidal references are provided by a *Phase-Locked-Loop* (PLL) scheme. Control was done using abc coordinates, facilitating controllers' designs for acting under unbalanced loads once they are simply replicated to the three loops. Current loops have high bandwidth (BW) (8 kHz), uses proportional-integral controllers and the three are identical. Current references i_{ref}^* are composed by four components:

TABLE I. MVQR Specifications

Parameter	Value
Nominal converter power	S_{conv} = 30 kVA
Grid voltage	V_{gd_pk} = 220 Vrms
dc-link total voltage	V_{total} = 800 V
dc-link total capacitance	$C_B = C_b/2$ = 7050 μF
Filter inductance	L_f = 560 μH
Filter capacitance	C_f = 47 μF
Current-sensor gain	K_i = 0.068
Voltage-sensor gain	K_v = 0.01
Triangular peak voltage	V_t = 11 V
Grid frequency	f_{gd} = 60 Hz
Switching frequency	f_s = 20 kHz
Sampling frequency	f_a = 20 kHz
Shunt resistance	R_{shunt} = 1 kΩ
Lf inductor series resistance	r_{Lf} = 0.1 Ω

- i_{dc}^* Continuous component used in unbalance compensation of dc-link differential voltage ($V_{b+} - V_{b-}$).
- i_0^* Direct component synchronized with v_{PCC}, where converter consumes needed active power for regulation of dc-link total voltage V_{total}.
- i_{90}^* Quadrature component synchronized with v_{PCC}, which is needed for reactive power circulation between converter and grid, promoting v_{PCC}-magnitude regulation.
- i_h^* Harmonic content, which are needed to complement non-linear load currents, hence reducing harmonic content echoed at v_{PCC}.

Harmonic controller is arranged using a sum of four resonant filters [10] centered at 3^{rd}, 5^{th}, 7^{th} and 9^{th} harmonics, which concentrate large amount of harmonic energy. Controller C_{Vh} receives the feedback from v_{PCC} and produces the harmonic-current reference (i_h^*) that mitigates harmonic voltages. Exclusively this controller was digitally implemented.

V_{total} is controlled using a PI controller (C_{total}) with BW around 6 Hz, not responding to natural oscillations of V_{total}. C_{total} controller's signal i_0' is multiplied by the PLL component that is in phase with v_{PCC}, producing i_0^*.

Differential dc-link voltage ($V_{dif} = V_{b+} - V_{b-}$) is controlled using a PI controller (C_{dif}) with 2 Hz BW, blocking signals which has grid's and upper frequencies. Controller C_{dif} produces the continuous-current reference i_{dc}^*.

PCC-voltage effective value (v_{PCC_rms}) is controlled using a PI controller (C_{rms}) with around 1 Hz BW, cutting off signals with grid's frequency. C_{rms} controller's signal is multiplied by the PLL component in quadrature with v_{PCC}, producing i_{90}^*.

MVQR parameters are presented in Table I.

Once the design of the controllers C_{total}, C_{dif} and C_{rms} are very similar to those implemented in [35], they are not discussed. These controllers are presented in Table II.

A. Boundary Conditions

This paper was based in a branch of a real distribution grid. The branch is 277 meters long from the transformer

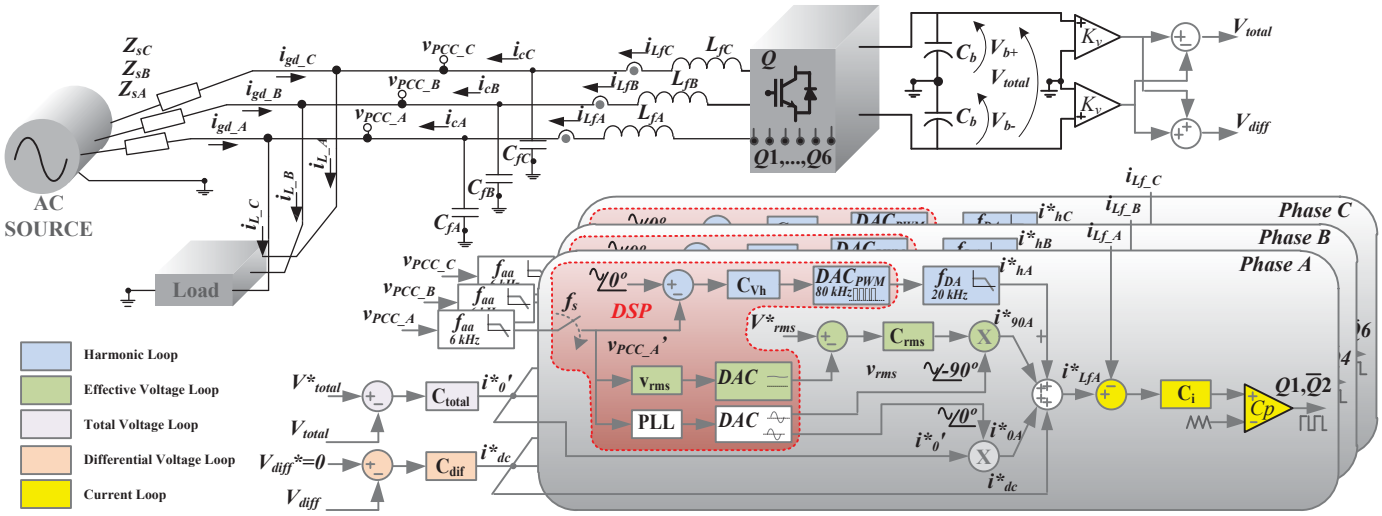

Fig. 2. General diagram of control loops.

TABLE II. CONTROLLERS C_{total}, C_{dif} AND C_{rms}

Controller	Transfer Function
$C_{total}\,(s)$	$-6\dfrac{s/2\pi 6+1}{s^2/2\pi 60+s}$
$C_{dif}\,(s)$	$3.3\dfrac{s/2\pi 2+1}{s^2/2\pi 20+s}$
$C_{rms}\,(s)$	$3100\dfrac{s/2\pi 2+1}{s^2/2\pi 13+s}$

TABLE III. PARAMETERS OF THE GRID

Parameter /Element	Impedance (Ω/Km)	Length (m)	R (max) (mΩ)	L (max) (μH)
Segment 1	$0.599+j0.467$	34	21	42.7
Segment 2	$1.485+j0.508$	243	361	327.5
Transf.	-	-	6.5	85.8
Param.(max)	-	**277**	**391**	**456**
Param.(min)	-	**0**	**6.5**	**85.8**

to the end of the longest branch and it has two segments as Fig. 1 presents. The grid's parameters are presented in Table III, where in the end of the branch the rate R/X_L is 2.3 and it can rise as the branch becomes longer or as the transformer becomes smaller. Designing controllers, the minimum and maximum grid's series impedance were respectively considered as in (1) and in (2), where necessary power for v_{PCC} compensation can be evaluated through the methodology presented in [36].

$$Z_{s\_L} = (50m + j \cdot 50\mu H \cdot 2\pi \cdot f_{gd})\Omega \tag{1}$$

$$Z_{s\_H} = (500m + j \cdot 500\mu H \cdot 2\pi \cdot f_{gd})\Omega \tag{2}$$

If the converter tries to exceed the limit of current which it is capable of injecting in grid, its output current i_c will be under non-linear effects due saturation of control action, thus the converter can contribute with v_{PCC} harmonic distortion instead of reducing it. Assuming that the maximum generable

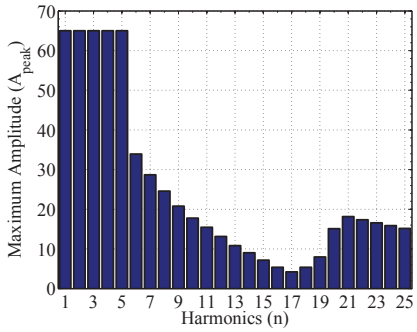

Fig. 3. Peak values of maximum current the converter is capable of generating for each harmonic according to (3) and considering the maximum grid impedance Z_{s_H}.

voltage at converter's output is $V_{total}/2$ and the maximum grid voltage is V_{gd_pk}, the maximum current the converter is capable of generating is approximately given by (3), where pwm modulator is considered as a gain and in (4) is described the current plant $G_i(s)$. In Fig. 3 is presented the maximum current for each harmonic and it already considers the transistors' limits.

$$I_{max}(n) = \left(\frac{V_{total}}{2} - V_{gd\_pk}\right)\frac{2V_t}{V_{total}}|G_i(j \cdot 2\pi \cdot f_{gd} \cdot n)| \tag{3}$$

$$G_i\,(s) = \frac{(V_{total}/2V_t)\left[s^2\,(L_sC_f) + s\,(r_sC_f) + 1\right]}{s^3\,(L_sL_fC_f) + s^2\,(L_fr_sC_f) + s\,(L_f + L_s) + r_s} \tag{4}$$

B. Current control

The converter topology, with neutral point connected to center of dc link, allows single-phase representation of its circuit as in Fig. 4, where i_L, v_{c_pwm}, r_s and L_s represent, respectively, load current, pwm-modulated voltage at one phase of the converter's output, equivalent series resistance and inductance of grid's path.

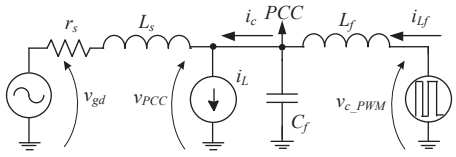

Fig. 4. Modeled circuit for harmonic plant as well as for current plant.

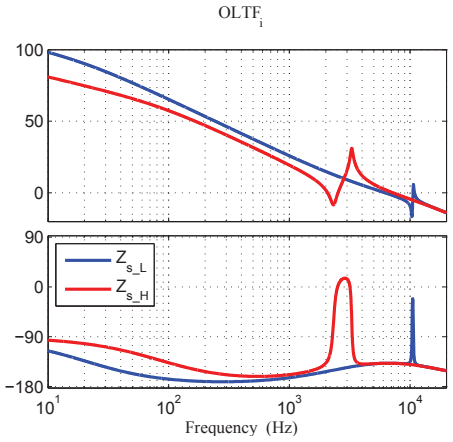

Fig. 5. Bode diagram of current OLTF with the proposed controller.

Current-plant model considers the pwm modulator (triangular carrier) as a simple gain, having a good fidelity upto around 15 kHz, which along with analog controller aids the plant stabilization once there is no phase delay before this frequency, allowing a larger BW. Situation that would be more complex if a zero-order holder with digital controller were used.

Current plant is shown in (4), where $G_i\,(s)$ represents the division i_{Lf} by duty cycle d. Also R_{shunt} and r_{Lf} were included in model of this design. In (5) is presented the designed current controller C_i.

$$C_i\,(s) = 4.2 \cdot 10^4 \cdot \left(\frac{\frac{s}{2\pi 400} + 1}{\frac{s^2}{2\pi 9000} + s} \right) \tag{5}$$

Figure 5 presents bode diagram of open-loop transfer function (OLTF) of current plant with the implemented current controller, for the minimum series impedance (Z_{s_L}) as well as the maximum (Z_{s_H}). Its BW is around 7 kHz, having a good disturbance rejection and reference tracking upto 1.5 kHz. Current controller is not required to provide null reference error once outer voltage controllers modify their references until they achieve a right control action, which is needed for MVQR operation. Only a PI controller was enough to turn the plant stable for the whole range of proposed parameter variation.

C. Voltage-harmonic control

A summation of resonant filters, at 3^{rd}, 5^{th}, 7^{th} and 9^{th} harmonics was designed for harmonic mitigation. In this controller's structure there is a zero at origin for blocking responses at dc and fundamental frequency. Also a signal in phase with v_{PCC}, coming from PLL, was used as its reference (v_h^*), reducing fundamental-frequency error and reducing the respective controller response.

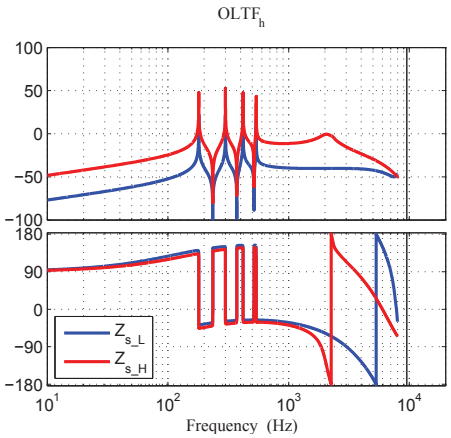

Fig. 6. Bode diagrams of harmonic OLTF with the proposed controller.

Harmonic loop gain was adjusted so that the OLTF is higher than 0 dB only at the frequencies of interest, reducing BW of this loop thus reducing dynamic of its transient response, becoming slower than current loop response, hence uncoupling both loops at the same time that it promotes v_{PCC} low-voltage-harmonic components in steady state. Transfer function of the voltage-harmonic controller (C_{Vh}) is presented in (6), where bilinear transformation was used to turn the controller discrete. The parameters of C_{Vh} controller are: $Q = 5000$, $K_h(k) = \{2.5; 1; 0.5; 0.15\}$ and $\omega_0 = 2\pi f_{gd}$.

$$C_{Vh}\,(s) = \sum_{k=3,5,7,9} K_h(k) \frac{s\frac{(k\omega_0)^2}{Q}}{s^2 + s\frac{k\omega_0}{Q} + (k\omega_0)^2} \tag{6}$$

Limitation of current reference amplitudes is desired once it also limits i_{Lf} independently of v_{PCC}'s amplitude, protecting the converter against damages. References i_{dc}^*, i_0^* and i_{90}^* are limited through limitation of their respective controller's outputs C_{dif}, C_{total} and C_{rms}. Nevertheless using the same technique for i_h^* limitation its amplitude will be either too high or too low according to Fig. 3. However the use of resonant filters allows an individual current limitation in (6), before summing all filters' control output. Thereby the use of maximum converter capacity still respecting the limits of (3) becomes possible. Despite this analysis this paper does not implement a saturation technique at resonant filters.

Voltage plant G_v is presented in (7) and bode diagrams of harmonic OLTFs are presented in Fig. 6, for the minimum series impedance (Z_{s_L}) as well as for the maximum (Z_{s_H}). They consider the whole current closed-loop transfer function (CLTF) in cascaded with the voltage plant.

$$G_v = \frac{v_{PCC}\,(s)}{i_{Lf}\,(s)} = \frac{sL_{gd} + r_{gd}}{s^2 C_f L_{gd} + sC_f r_{gd} + 1} \tag{7}$$

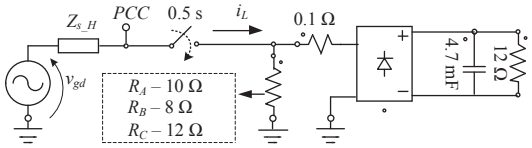

Fig. 7. Single-phase load circuit which was used to simulate the proposed control scheme.

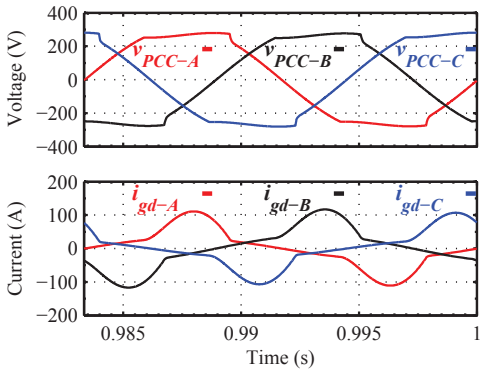

Fig. 8. PCC voltages (v_{PCC}) and grid currents (i_{gd}) (which are identical to i_L) without MVQR. Effective values of voltages at phases A, B and C are respectively 208.5 V, 206.8 V and 210.1 V.

D. Interaction among control loops

Differential-voltage loop produces a dc current level which practically does not modify PCC's voltage magnitude, does not charge the dc link and does not produce harmonics. Total-voltage loop produces i_d, which does not unbalance the dc link, does not produce harmonics and practically does not modify v_{PCC} amplitude. Control action of v_{PCC} control loop does not modify amplitude or balance of the dc link and does not produce harmonics, therefore it also does not interact with others loops. The harmonic loop also does not modify neither dc-link average voltages nor fundamental components of PCC. Thus, just designing voltage loops much slower than the current loop is enough to decouple all loops, facilitating controllers' design. However, in the case of the PLL does not have a good performance interaction between loops which act in fundamental components becomes possible.

III. Simulation Results

Aiming to verify the operation of all control scheme, the whole circuit was simulated using the software PSIM for the lager grid equivalent series impedance Z_{s_H} and the load presented in Fig. 7, where resistances R_A, R_B and R_C cause unbalance among the phases A, B and C, the remainder circuit is replicated to the three phases. The load has linear (resistance) and nonlinear (diodes rectifier with capacitor filter) parts, where it is switched in 0.5 seconds. This section presents system's voltages and currents, using and not using MVQR, harmonic analysis of phase C and converter behavior during load transient at 0.5 s.

v_{PCC} voltages and i_{gd} currents (which are identical to i_L with and without MVQR, are presented in Fig. 8. It is noticed the maximum load current is around 100 A.

v_{PCC}, grid currents (i_{gd}), i_L and converter currents (i_c), with MVQR are presented in Fig. 9. It is noticed the maximum load current is around 200 A, that is much higher than i_L without MVQR. It occurs because of peak-voltage increasing, which is promoted by converter's low impedance for load harmonics. Grid's phase C provides power of 10.4 kVA, power factor (PF) of 0.99, meanwhile the load consumes 13.1 kVA, PF of 0.78, and the MQVR processes 7.9 kVAr to regulate voltage magnitude and voltage harmonics at PCC.

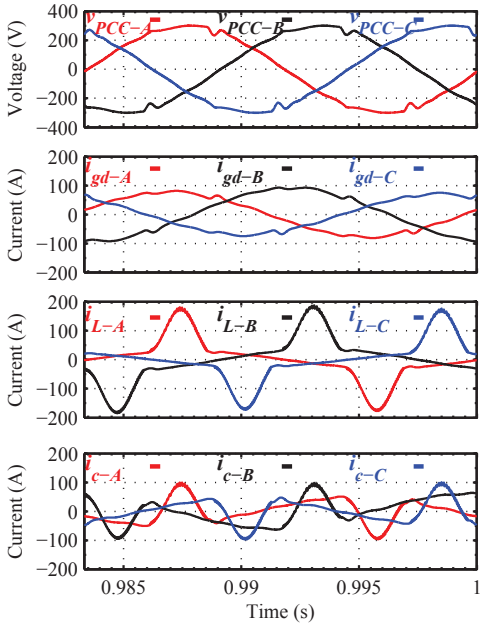

Fig. 9. PCC voltage (v_{PCC}), grid current (i_{gd}), load current (i_L) and converter current (i_c) of system with MVQR. All PCC voltages are regulated at 209,7 V.

TABLE IV. Simulation results of THD of voltage at point of connection (v_{pcc})

Parameter /Element	v_{PCC} THD WITHOUT MVQR (%)	v_{PCC} THD WITH MVQR (%)
Phase A	8.4	3.6
Phase B	8.4	3.4
Phase C	8.5	3.8

The sum of converter harmonic currents with nonlinear load current (rectifier) is approximately a sinusoidal current, but converter harmonic currents are composed by four harmonic components in spite of the greater number of harmonic components of nonlinear load current. Thus at the very moment the rectifier current becomes zero (E.g. at 0.9885 s to phase A), i_{Lf} current does not keep up with such high derivative and once converter's current is becoming negative the grid current is also momentously increased (see polarity), so that promoting momentary voltages sags in PCC voltage.

In Table IV is represented a large THD reduction when inserting the MVQR, recalling that inserting the MVQR harmonic currents rises considerably, which can be noticed through an increasing of rectifier's peak current.

In Fig. 10 is presented upto the 25^{th} harmonic components of the currents i_{gd}, i_L and i_c of phase C. It can be noticed

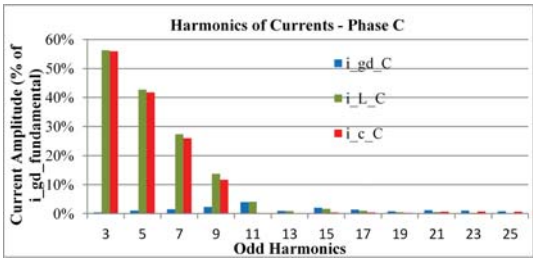

Fig. 10. Harmonic analysis of grid current i_{gd} in blue, load current i_L in green and converter current in red.

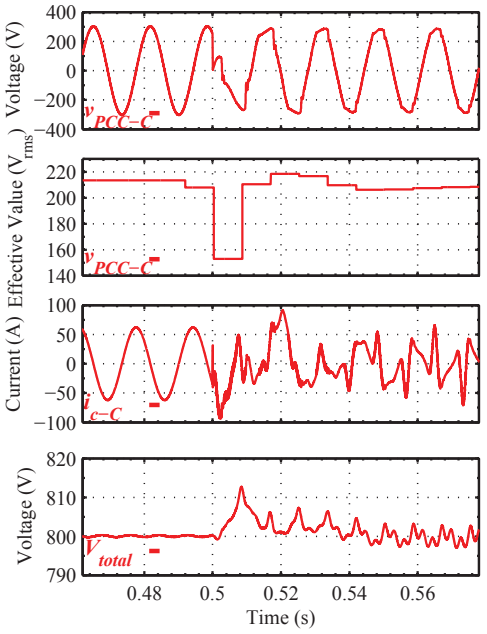

Fig. 11. Instantaneous and effective values of v_{PCC} (phase C), i_c (phase C) and V_{total} during load insertion.

there is very low harmonic circulation in grid path, it becomes possible once load harmonics are drained by the MVQR (upto the 9^{th} harmonic) once they have almost the same amplitude.

MVQR behavior under transients is presented in Fig. 11 with instantaneous and effective values of v_{PCC}, with i_c and with dc-link total voltage (V_{total}) during load insertion at 0.5 s. Initially v_{gd} is higher than MVQR-voltage reference (V^*_{rms}) therefore v_{PCC} is compensated with inductive reactive power until load connection. After this moment it is noticed that the effective voltage at PCC is regulated in a period much lower than 3 seconds that is required by ANEEL standard, thus this value is classified as adequate although its momentary voltage sag (0.68 pu (150 V) at 0.5 s). v_{PCC} effective value is calculated cycle-by-cycle, so that the measurement presents steps. The reduced dynamics of harmonic loop allows only 100 A of converter peak current during this transient, which is not excessive. V_{total} was kept regulated and it had a ripple correspondent to MVQR harmonic compensation.

IV. Preliminary Experimental Results

In Fig. 12 is presented preliminary experimental results of harmonic loop for one phase, without reactive compensation,

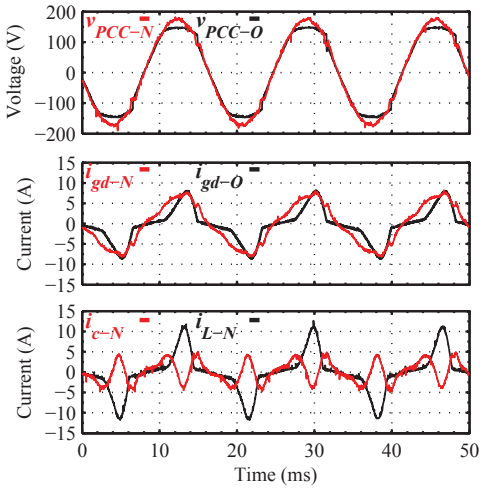

Fig. 12. Experimental results of v_{PCC} and i_{gd} with (v_{PCC-N}, i_{gd-N}) and without (v_{PCC-O}, i_{gd-O}) MVQR and of i_c and i_L with MVQR.

with reduced power and reduced voltage. It presents v_{PCC} and i_{gd} using and not using MVQR and presents i_c and i_L with MVQR. These results prove that this control technique works, once the THD changed from 8.6% to 3.3% with MVQR insertion.

V. Conclusions

In this paper was presented a control scheme for DSTATCOM current controlled that was used for voltage magnitude regulation at point of common coupling (PCC) through reactive injection, also it mitigates voltage harmonics through PCC voltage detection. In this paper there are all control schemes of this solution, an analysis of physical limits of grid current injection, the current and PCC voltage plant models, controller's designs, simulation results of the complete system using nonlinear loads and preliminary experimental results.

Voltage harmonic mitigation without current measurements at load or source branches turns the solution feasible, because there is no necessity of awareness of the exact location of harmonic sources. It is done through resonant filters that produce needed current references to compensate load harmonics near a PCC, where a PI current controller is enough to track that references. Using a fundamental voltage signal as harmonic-loop reference allows non-inclusion of a notch filter in harmonic-controller design.

A harmonic analysis validates the effectiveness of the control strategy, where the load-harmonic content were almost totally eliminated at 3^{rd}, 5^{th}, 7^{th} and 9^{th} harmonics. Preliminary experimental results demonstrated the success of the technique.

Capacity of voltage regulation through reactive power was kept as well as dc-link voltage regulation.

The total power of the used load is acceptable for this grid model once in a real situation there is power sharing among grid's branches.

Acknowledgments

The authors are glad for the support of FITEJ, FAPESC, CAPES and CELESC, which turned this paper feasible.

REFERENCES

[1] *Procedimentos de Distribuição de Energia Elétrica no Sistema Elétrico Nacional - PRODIST*, Agência Nacional de Energia Elétrica Std., Rev. 5, 2014.

[2] *IEEE Recommended Practices and Requirements for Harmonic Control in Electric Power Systems*, IEEE 519 Std.

[3] H. Akagi, "New trends in active filters for improving power quality," in *Power Electronics, Drives and Energy Systems for Industrial Growth, 1996., Proceedings of the 1996 International Conference on*, vol. 1, Jan 1996, pp. 417–425 vol.1.

[4] J. Rocabert, A. Luna, F. Blaabjerg, and P. Rodríguez, "Control of power converters in ac microgrids," *Power Electronics, IEEE Transactions on*, vol. 27, no. 11, pp. 4734–4749, Nov 2012.

[5] A. Chandra, B. Singh, B. Singh, and K. Al-Haddad, "An improved control algorithm of shunt active filter for voltage regulation, harmonic elimination, power-factor correction, and balancing of nonlinear loads," *Power Electronics, IEEE Transactions on*, vol. 15, no. 3, pp. 495–507, May 2000.

[6] Y. A. R. I. Mohamed and E. El-Saadany, "A control scheme for pwm voltage-source distributed-generation inverters for fast load-voltage regulation and effective mitigation of unbalanced voltage disturbances," *Industrial Electronics, IEEE Transactions on*, vol. 55, no. 5, pp. 2072–2084, May 2008.

[7] C. A. C. Cavaliere, "Análise e modelagem de statcom considerando operação em sistema desbalanceado," Ph.D. dissertation, COPPE/UFRJ, Fevereiro 2008, cOPPE.

[8] M. Aggarwal, S. K. Gupta, M. Madhusudan, and G. Kasal, "D-statcom control in low voltage distribution system with distributed generation," in *Emerging Trends in Engineering and Technology (ICETET), 2010 3rd International Conference on*, Nov 2010, pp. 426–429.

[9] B. Singh, A. Adya, A. Mittal, and J. R. P. Gupta, "Analysis, simulation and control of dstatcom in three-phase, four-wire isolated distribution systems," in *Power India Conference, 2006 IEEE*, 2006, p. 6 pp.

[10] P.-C. Tan, R. Morrison, and D. Holmes, "Voltage form factor control and reactive power compensation in a 25-kv electrified railway system using a shunt active filter based on voltage detection," *Industry Applications, IEEE Transactions on*, vol. 39, no. 2, pp. 575–581, Mar 2003.

[11] J. Miret, M. Castilla, J. Matas, J. Guerrero, and J. Vasquez, "Selective harmonic-compensation control for single-phase active power filter with high harmonic rejection," *Industrial Electronics, IEEE Transactions on*, vol. 56, no. 8, pp. 3117–3127, Aug 2009.

[12] P. Mattavelli and F. Marafao, "Repetitive-based control for selective harmonic compensation in active power filters," *Industrial Electronics, IEEE Transactions on*, vol. 51, no. 5, pp. 1018–1024, Oct 2004.

[13] R. Costa-Castelló?, R. Grino, and E. Fossas, "Odd-harmonic digital repetitive control of a single-phase current active filter," *Power Electronics, IEEE Transactions on*, vol. 19, no. 4, pp. 1060–1068, July 2004.

[14] G. Weiss, Q.-C. Zhong, T. Green, and J. Liang, "H infin; repetitive control of dc-ac converters in microgrids," *Power Electronics, IEEE Transactions on*, vol. 19, no. 1, pp. 219–230, Jan 2004.

[15] H. Akagi, "Control strategy and site selection of a shunt active filter for damping of harmonic propagation in power distribution systems," *Power Delivery, IEEE Transactions on*, vol. 12, no. 1, pp. 354–363, Jan 1997.

[16] F. Freijedo, J. Doval-Gandoy, O. Lopez, P. Fernandez-Comesana, and C. Martinez-Penalver, "A signal-processing adaptive algorithm for selective current harmonic cancellation in active power filters," *Industrial Electronics, IEEE Transactions on*, vol. 56, no. 8, pp. 2829–2840, Aug 2009.

[17] H. Akagi, H. Fujita, and K. Wada, "A shunt active filter based on voltage detection for harmonic termination of a radial power distribution line," in *Industry Applications Conference, 1998. Thirty-Third IAS Annual Meeting. The 1998 IEEE*, vol. 2, Oct 1998, pp. 1393–1399 vol.2.

[18] M. Salo and H. Tuusa, "A novel open-loop control method for a current-source active power filter," *Industrial Electronics, IEEE Transactions on*, vol. 50, no. 2, pp. 313–321, Apr 2003.

[19] Y. Sato, H. Chigira, and T. Kataoka, "A new control method for active power filters with voltage detection," in *Power Conversion Conference - Nagaoka 1997., Proceedings of the*, vol. 1, Aug 1997, pp. 169–174 vol.1.

[20] H. Akagi, "Active harmonic filters," *Proceedings of the IEEE*, vol. 93, no. 12, pp. 2128–2141, Dec 2005.

[21] M. Aredes and L. F. C. Monteiro, "A control strategy for shunt active filter," in *Harmonics and Quality of Power, 2002. 10th International Conference on*, vol. 2, Oct 2002, pp. 472–477 vol.2.

[22] Y. Sato, T. Kawase, M. Akiyama, and T. Kataoka, "A control strategy for general-purpose active filters based on voltage detection," *Industry Applications, IEEE Transactions on*, vol. 36, no. 5, pp. 1405–1412, Sep 2000.

[23] A. Etemadi and R. Iravani, "Overcurrent and overload protection of directly voltage-controlled distributed resources in a microgrid," *Industrial Electronics, IEEE Transactions on*, vol. 60, no. 12, pp. 5629–5638, Dec 2013.

[24] C. Gehrke, A. Lima, and A. Oliveira, "Controlling harmonics in electrical power systems for satisfying total and individual harmonic distortion constraints," in *Applied Power Electronics Conference and Exposition (APEC), 2014 Twenty-Ninth Annual IEEE*, March 2014, pp. 3342–3348.

[25] J. He, Y. W. Li, F. Blaabjerg, and X. Wang, "Active harmonic filtering using current-controlled, grid-connected dg units with closed-loop power control," *Power Electronics, IEEE Transactions on*, vol. 29, no. 2, pp. 642–653, Feb 2014.

[26] C. Kumar and M. Mishra, "A multifunctional dstatcom operating under stiff source," *Industrial Electronics, IEEE Transactions on*, vol. 61, no. 7, pp. 3131–3136, July 2014.

[27] R. Mastromauro, M. Liserre, and A. Dell'Aquila, "Control issues in single-stage photovoltaic systems: Mppt, current and voltage control," *Industrial Informatics, IEEE Transactions on*, vol. 8, no. 2, pp. 241–254, May 2012.

[28] Y. A. R. I. Mohamed and E. El-Saadany, "Hybrid variable-structure control with evolutionary optimum-tuning algorithm for fast grid-voltage regulation using inverter-based distributed generation," *Power Electronics, IEEE Transactions on*, vol. 23, no. 3, pp. 1334–1341, May 2008.

[29] Y.-R. Mohamed, "Mitigation of dynamic, unbalanced, and harmonic voltage disturbances using grid-connected inverters with lcl filter," *Industrial Electronics, IEEE Transactions on*, vol. 58, no. 9, pp. 3914–3924, Sept 2011.

[30] S. Arya, B. Singh, A. Chandra, and K. Al-Haddad, "Power factor correction and zero voltage regulation in distribution system using dstatcom," in *Power Electronics, Drives and Energy Systems (PEDES), 2012 IEEE International Conference on*, Dec 2012, pp. 1–6.

[31] D. Vilathgamuwa, P. C. Loh, and Y. Li, "Protection of microgrids during utility voltage sags," *Industrial Electronics, IEEE Transactions on*, vol. 53, no. 5, pp. 1427–1436, Oct 2006.

[32] T.-L. Lee and S.-H. Hu, "Discrete frequency-tuning active filter to suppress harmonic resonances of closed-loop distribution power systems," *Power Electronics, IEEE Transactions on*, vol. 26, no. 1, pp. 137–148, Jan 2011.

[33] S.-L. Jung, H.-S. Huang, M.-Y. Chang, and Y.-Y. Tzou, "Dsp-based multiple-loop control strategy for single-phase inverters used in ac power sources," in *Power Electronics Specialists Conference, 1997. PESC '97 Record., 28th Annual IEEE*, vol. 1, Jun 1997, pp. 706–712 vol.1.

[34] A. Yepes, F. Freijedo, J. Doval-Gandoy, O. Lopez, J. Malvar, and P. Fernandez-Comesana, "On the discrete-time implementation of resonant controllers for active power filters," in *Industrial Electronics, 2009. IECON '09. 35th Annual Conference of IEEE*, Nov 2009, pp. 3686–3691.

[35] J. da Cunha, W. de Oliveira Rossi, A. Batschauer, and M. Mezaroba, "A simple control scheme to a voltage regulator based in a current controlled statcom," in *Power Electronics Conference (COBEP), 2013 Brazilian*, Oct 2013, pp. 1212–1218.

[36] T. P. Enderle, G. da Silva, C. Fischer, R. C. Beltrame, L. Schuch, V. F. Montagner, and C. Rech, "D-statcom applied to single-phase distribution networks: Modeling and control," in *IECON 2012 - 38th Annual Conference on IEEE Industrial Electronics Society*, Oct 2012, pp. 321–326.